Designing Cross-Coupled Microstrip Bandpass Filter Based Coupling Matrix Optimization Technique

Damou Mehdi, Chetioui Mohammed, Mustafa Secmen,
Boudkhil Abdelhakim, Gouni Slimane

*Abstract –***This research article presents a novel compact cross-coupled bandpass filter (BPF) microstrip operating at 1.2 GHz. The proposed filter is designed and developed by coupling the RLC resonator and TL transmission line circuits, excited by a symmetrical microstrip feed line (MSL). The fractional bandwidth (FBW) of the filter is found to be 12.83%. The equivalent lumped circuit model of the filter is obtained from AWR Designer. By decomposing the filter into separate entities for individual electromagnetic (EM) simulation via the High Frequency Structure Simulator (HFSS) and the equivalent lumped circuit model of the filter is obtained in AWR designer, this approach achieves computational efficiency, facilitating the extraction of key parameters aligned to specified general coupling matrix (CM). All these parameters from the overall response of the filter are used in the Chebychev approximation method models at the second and fourth order. The transmission zeros are close to the bandpass edge. The proposed filter has a reflection loss($|S_{11}|$) less than -25 dB and an insertion loss (-$|S_{21}|$) less than 0.21dB. Besides, the filter has strong and varying group delay response over the entire bandwidth from 1.15 GHz to 1.3 GHz. The proposed bandpass filter also shows good stopband rejection (being greater than 25 dB) and $|S_{11}|$< -0.1 dB from 1.35 GHz to 1.75 GHz and sharp decrease in bandwidth at the hard shoulder. All simulated results are extracted via the HFSS simulator method based on finite element, FEM. All results produced by AWR design software have a close similarity with the results simulated and optimized by HFSS.**

Keywords: **Microstrip, Bandpass filter, Coupling Matrix, Cross-Coupled, HFSS.**

I. INTRODUCTION

Recently, significant advancements have been made in using computer-aided design (CAD) tools for designing RF/microwave circuits, especially in simulating full-wave

Damou Mehdi, Chetioui Mohammed, Boudkhil Abdelhakim and Gouni Slimane are with the Laboratory of Electronics, Advanced Signal Processing and Microwave -University of Saida Dr Moulay Tahar, - BP 138- Ennasr, Saida-Algeria, E-mails: bouazzamehdi@yahoo.fr, boudkhil.abdelhakim@yahoo.fr, chetioui.mohammed@yahoo.fr, ameurdz679@gmail.com.

Mustafa Secmen is with the Department of Electrical and Electronics Engineering, Yasar University, University Street, No: 37-39 , Agacli Yol, 35100, Bornova, Izmir, Turkey, E-mail: mustafa.secmen@yasar.edu.tr

electromagnetic (EM) waves. These advancements have been integrated into commercial and proprietary software that is now pivotal for simulating, modeling, designing, and validating microwave filters. Planar bandpass filters have become critical for many modern wireless communication systems due to their compactness, which is essential due to space constraints. The half-wavelength open-loop resonator inherently has a spurious pass band at twice the resonant frequency ($2f_0$) [1], while the first spurious frequency for the quarter-wavelength resonator filter appears at three times the resonant frequency ($3f_0$) and requires a short-circuit via a cavity for operation. Historically, research has focused on various strategies to reduce spurious pass band in filters, with notable approaches including the use of microstrip parallel coupled lines [1]. It's been recommended that to adjust for phase velocity differences, parallel-coupled microstrip filters with over-coupled end stages should be employed to extend the electric length of the odd mode. The research has also explored the wiggly line microstrip filter [1], which uses a continuous sinusoidal alteration in the width of the coupled lines governed by a sinusoidal law, and parallel-coupled microstrip filters that manage the spurious signal in the stopband by adjusting the width of perforations in the ground plane. A substrate suspension structure was proposed to enhance even-mode phase velocity and balance modal phase velocities for better spurious band suppression. For moving the spurious band to higher frequencies using step impedance resonators (SIR), a significant impedance ratio is necessary. This paper presents the design and optimization of a 2nd and 4th-order bandpass microstrip cross-coupled filter using a coupling matrix with a fractional bandwidth of 15.84% [2]. The design process utilizes HFSS and AWR simulators to create an electromagnetic filter model based on a Chebyshev lowpass prototype with frequency transformation, allowing for direct tuning of the filter's resonant frequency, coupling coefficients, and external quality factor. The methodology for determining the microstrip filter dimensions and designing the proposed structures is thoroughly discussed to enhance filter selectivity through transmission zeros.

II. COUPLING MATRIX THEORY

It should be noted that the coupling matrix has the capability to incorporate certain practical characteristics of the filter elements. Every individual element within the matrix can be distinctly associated with a specific element in the final microwave device [3]. This allows for the attributions of the electrical properties of individual elements, including the quality factor Q_e values associated with each resonator cavity, to be accounted for.
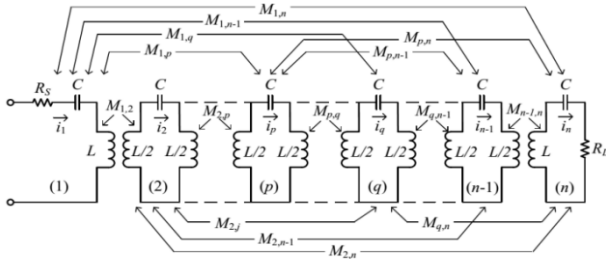
Fig. 1. A typical series-resonator bandpass network

The equivalent circuit with magnetically coupled resonators is given in Fig.1. Using Kirchhoff's voltage law, the coupling matrix is derived via an impedance matrix from a set of loop equations. The other circuit with electrical coupling is given in Fig. 2 (b) [4]. The coupling matrix is derived via an admittance matrix formulated by a set of node equation based on Kirchhoff's current law. Regardless of the type of coupling, a general matrix [**A**] formed by coupling coefficients $m_{p,q}$ and external quality factors q_{ei} is presenteddin as:

$$[\mathbf{A}] = [\mathbf{q}] + p[\mathbf{U}] - j[\mathbf{m}],$$

$$[\mathbf{A}] = \begin{bmatrix} \frac{1}{q_{e1}} & 0 & \cdots & 0 \\ 0 & 0 & & 0 \\ \vdots & & \ddots & \vdots \\ 0 & & \cdots & \frac{1}{q_{en}} \end{bmatrix} + p \begin{bmatrix} 1 & 0 & \cdots & 0 \\ 0 & 1 & & 0 \\ \vdots & \vdots & \cdots & \vdots \\ 0 & 0 & \cdots & 1 \end{bmatrix} - j \begin{bmatrix} m_{1,1} & m_{1,2} & \cdots & m_{1,n} \\ m_{2,1} & m_{2,2} & & m_{2,n} \\ \vdots & \vdots & \cdots & \vdots \\ m_{n,1} & m_{n,2} & \cdots & m_{n,n} \end{bmatrix}, (1)$$

$$p = j \frac{1}{FBW} \left(\frac{\omega}{\omega_0} - \frac{\omega_0}{\omega} \right),$$

where matrix [**U**] is an identity matrix, p is the complex lowpass frequency variable, ω_0 is the centre frequency of the filter, *FBW* is the fractional bandwidth of the filter, q_{ei} (i=1 and n) is the scaled external quality factors of the resonator i. $m_{p,q}$ is the normalised coupling coefficients between the resonator p and q. As given in formula (2), the *S*-parameters can be calculated using the scaled external quality factors q_{ei} (i=1 and n) and matrix [**A**] as:

$$S_{11} = \pm \left(1 - \frac{2}{q_{e1}} [\mathbf{A}]_{1,1}^{-1} \right),$$

$$S_{21} = 2 \frac{1}{\sqrt{q_{e1} \cdot q_{en}}} [\mathbf{A}]_{n,1}^{-1}. \tag{2}$$

A.   Physical realization of coupling matrix

After determining the normalized coupling matrix [m] for a coupled resonator topology, the actual coupling matrix [M] of a coupled resonator device with given specification can be calculated by prototype de-normalization of the matrix [m] at a desired bandwidth, as follows [5]:

$$Q_{es} = \frac{g_0 g_1}{FBW}, \ \ Q_{eL} = \frac{g_n g_{n+1}}{FBW}, \tag{3}$$

$$M_{i,i+1} = \frac{FBW}{\sqrt{g_i g_{i+1}}}, \ \ i = 1 \ to \ n-1, \tag{4}$$

$$m_{i,i+1} = \frac{M_{i,i+1}}{FBW}, \ \ i = 1 \ to \ n-1. \tag{5}$$

B.   Band pass filter based on an electronic circuit

The design of bandpass filters based on electronic circuits is based on the following steps:

- Specifications: filter type, filter order n, filter ripple level, filter bandwidth *BW*, relative bandwidth *FBW*, cutoff frequency and center frequency
- Determination of the values of the elements g_i .
- Calculation of the coupling elements $M_{(i,i+1)}$ and the external quality factors (Q_{ext} and Q_{in}) which are linked to the elements g_i .
- Calculation of the lumped elements $R_0 L_0 C_0$ of resonators.
- Calculation of impedances in series of equivalent circuit with lumped elements.

III.   DESIGN SPECIFICATIONS AND INITIAL MICROSTRIP FILTER MODEL

The specifications imposed for this filter are as Table 1, the circuit will be synthesized is defined in Environment as distributed element bandpass filter.

TABLE 1.   THE FOLLOWING SPECIFICATIONS OF THE FILTER

Function	Chebyshev
Order	$N=4$
Center Frequency	1.2dGHz
LAr (passband ripple)	0.04321 dB
Bandwidth at -3 dB	BW=154.1MHz
Reflection loss: RL	$< - 20$ dB
TFZ	f_{zt1}=1.08 GHz and f_{zt2}=1.37 GHz

Once the order of the filter is determined [6], knowing the maximum ripple of 0.04321 dB and the specifications defined in the specifications, we obtain the coefficients *gi* (i=1-4) of the band-pass prototype of the type filter Chebyshev:

g_0	g_1	g_2	g_3	g_4	g_5
1	0.9314	1.2920	1.5775	0.7628	1.2210

Using the specifications defined in the design, the calculated values for relative bandwidth, quality factor and coupling coefficients are given in formulas (6)-(7) and in below table.

$$\omega_0 = 2\pi f_0, \ \ FBW = \frac{BW}{f_0} = 12.84\%, \tag{6}$$

$$Q_e = \frac{g_0 g_1}{FBW} = \frac{1 * 0.9314}{0.1284} = 7,253 \ . \tag{7}$$

Coupling coefficients

M_{12}	M_{23}	M_{34}	M_{14}
0.1099	0.1229	0.1099	-0.0282

Fig. 2. Coupling diagram of the 4th order filter

The four-pole microstrip cross-coupled filter is designed based on the following prescribed general coupling matrix:

$$[\mathbf{m}] = \begin{bmatrix} 0 & 0.8559 & 0 & -0.2196 \\ 0.8559 & 0 & 0.9571 & 0 \\ 0 & 0.9571 & 0 & 0.8559 \\ -0.2196 & 0 & 0.8559 & 0 \end{bmatrix}.$$

A. Equivalent circuit of the filter:

The equivalent lumped circuit mode of the proposed BPF shown in Figure 3 is shown in Figure 4. The results of the equivalent lumped circuit model are obtained using the circuit model tool of Ansoft design. Considering the layout of the proposed BPF, an equivalent circuit diagram is designed. The values of the grouped elements are manually optimized by changing the value of each element so that it can have good agreement with the simulated results obtained from the full wave simulator. In the lumped equivalent diagram, mutual coupling between individual elements is not considered. The impedance parameters, Z_{01} and Z_{45}, are generated by the transmission lines powered by input and output MSL. The three impedances Z_{12}, Z_{23} and Z_{34} are introduced due to the transmission lines. The left shunt inductors (L_i) are generated due to the short circuit of the input and output pads with ground plane. Straight shunt capacitances (C_i) are introduced to the parasitic effects of shorted stubs ground plane.
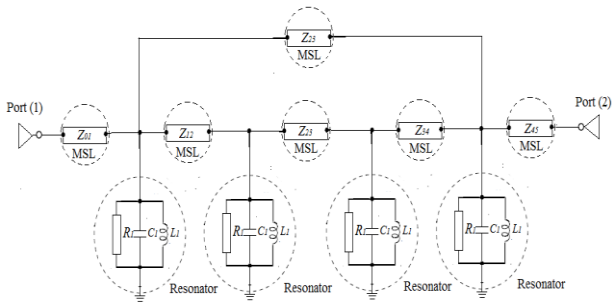
Fig. 3. Band pass filter with lumped elements of order 4 with circuit resonant $R_1L_1C_1$ parallel

Lumped elements (R_1, L_1, C_1) of resonators are given as [7]:

$$L_1 = \frac{Z}{\omega_0 Q_e} * 10^9 \text{ nH} = 0.88731 \text{ nH}, \qquad (8)$$

$$C_1 = \frac{Z}{\omega_0 Q_e} * 10^{12} \text{ pF} = 19.824 \text{ pF}, \qquad (9)$$

$$R_1 = 100000 \ \Omega. \qquad (10)$$

The impedances of the resonators are given as:

$$Z_{i,i+1} = \frac{Z}{Q_e M_{i,i+1}}. \qquad (11)$$

When $Z_0 = 50 \ \Omega$ is the supply impedance at the ports, the impedances of the resonators are calculated to be $Z_{12} = 60.86 \ \Omega, Z_{23} = 54.45 \ \Omega, Z_{34} = 60.86 \ \Omega, Z_{14} = -237.16 \ \Omega$.

The ideal transmission and reflection responses of the equivalent circuit in lumped elements analyzed with AWR are shown in Fig. 4. It appears that the frequency of our bandpass filter has center frequency at the 1.2 GHz. The filter is a narrow band 154.1 MHz, which presents reflection losses less than -20 dB in this band.
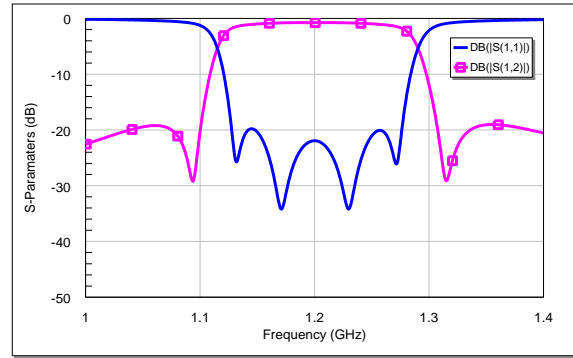
Fig. 4. Ideal response of the 4th order bandpass filter with lumped elements by quarter wave line

B. EM design of the band pass filter in planar technology

The topology of our band pass filter of order 4 is presented in the Fig. 5, which operates in the L-band frequency range and consists of four folded quarter-wave resonators with a length of folded wave, resulting in a compact filter topology on a dielectric substrate of thickness denoted by h. The filter has a short circuit (via-hole grounding) at one end and an open circuit at the other end. Resonators 1 and 4 are the input and output (I/O) resonators, respectively, and there is cross coupling between them. The microstrip bandpass filter (BPF) of the receiver will be studied, evaluated, constructed and simulated using the microstrip lines operating at 1.2 GHz with a 3 dB fractional bandwidth of 12.84%. The BPF is suitable for receiving 4G communication systems with a low frequency at 1.13 GHz and a high frequency at 1.28 GHz.
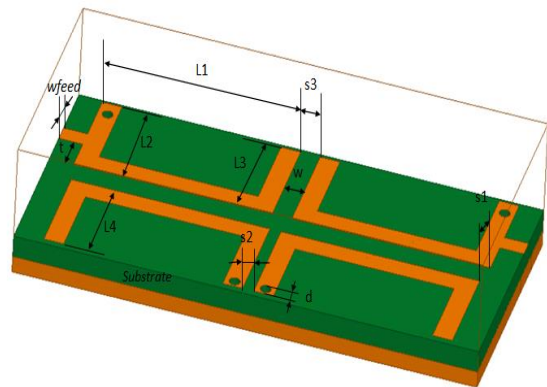
Fig. 5.3D structure of four-pole cross-coupled microstrip resonator filter

C. The filter dimensions

When the design of a microstrip filter involves full-wave EM simulations, it is computationally preferable to decompose the filter into different parts which are individually simulated by the EM simulator to extract the desired design parameters by function of a general coupling matrix[8]. They are then combined to obtain the response of the global filter. This CAD approach, whichh is particularly effective for the design of narrowband filters, is demonstrated with a four-pole cross-coupled filter, shown in Fig. 6.

The substrate Rogers (RO4003C) used in the design has a relative dielectric constant of $\varepsilon_r = 3.55$ and a substrate thickness of $h = 0.813$ mm. The filter configuration has a characteristic impedance of a microstrip line of $Z_0 = 50\ \Omega$, a copper line thickness of $T = 0.017$ mm, and a dielectric loss tangent $\tan \delta = 0.0027$. With the materials indicated here, the dimensions of the designed microstrip band-pass filter are given in Table 2.

TABLE 2.
DIMENSIONS OF THE MICROSTRIP BAND-PASS FILTER OF ORDER FOUR (N=4).

Parameters	x_1	y_1	H	H_s	L_1	L_2	L_3
	L_4	s_1	s_2	s_3	T	W_{feed}	w
Values	25	52	0.017	0.813	10.9	11	22
	10.5	0.9	0.25	1.13	2.3	2	2

D. External Quality Factor (Qe) Calculation by group delay

Another important step in filter design is the calculation of the external quality factor (Q_e). Input and output (I/O) resonators are connected by a tapped microstrip line to external 50 Ω terminations as can be seen in both Fig. 7. As a consequence, the width of the tapped strip (W_{feed}), its length (L_{feed}) as well as the feed position (t) (Fig. 8), they all play a significant role in determining Q_e. For implicity, W_{feed}=11 mm, is uniformly set for the filters presented in this paper. The other two variables are estimated from Fig. 8, which plots Q_e against 't'.
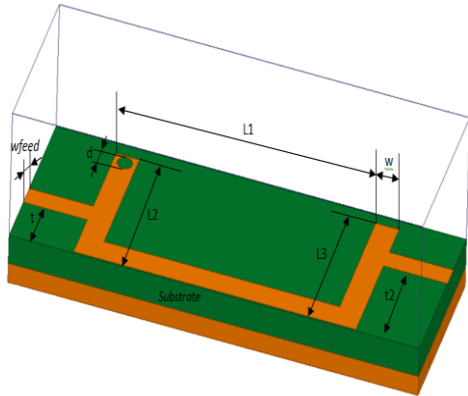
Fig. 7. Implementation for extraction of the external quality factor
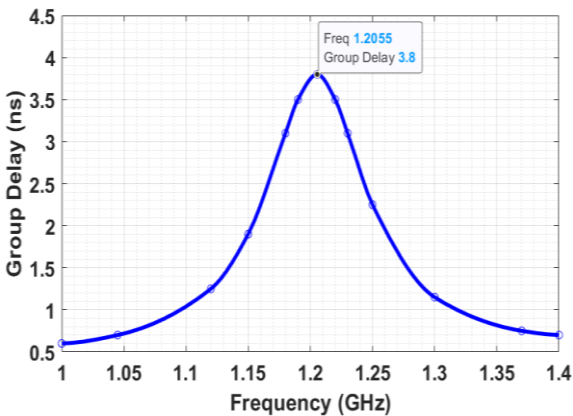
Fig. 8. Group delay of a microstrip resonator for quality factor sizing

The Q_e in Fig. 8 is extracted from the frequency response of a singly loaded I/O resonator [9]. FEM simulations of the tapped resonator depicted in Fig. 8 are carried out in HFSS. The Group delay provides the data for Q_e calculation using the formula given in (12).

$$Q_e = \frac{\omega_0 \tau_{s_{11}}(\omega_0)}{4} = \frac{2\pi \times 3.8 \times 1.2055}{4} = 7.1920. \quad (12)$$

Table 3 presents the values of several iterations to calculate the quality factor by varying the port location indicated in the given table:

TABLE 3.
DIMENSIONS AND PARAMETERS IN THE EXTRACTION

t	f_0(GHz)	τ	Q_e
0.2	0.9609	1.9	2.8678
0.4	1.0672	2.72	4.5597
0.6	1.0852	2.78	4.7389
0.8	1.1273	2.83	5.0112
1	1.119	4.15	7.2965
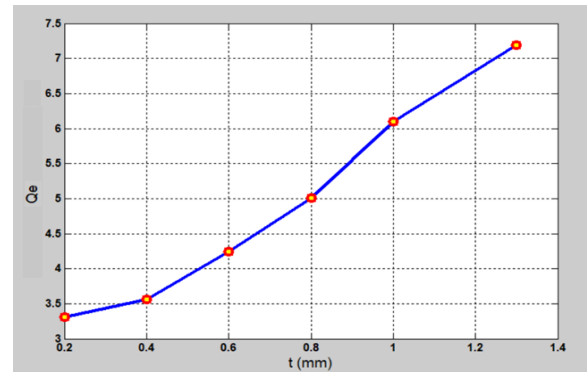
Fig. 9. External Quality Factor (Qe) vs the tapped microstrip position (t)

Fig. 9 represents the results of Table 3. A design of the curve of Q_e against t can be obtained, as shown in (Fig. **9**). In this case, as t increases, the branch line is moved towards the short circuit (via-hole grounding) of the resonator and therefore the coupling of the source is weaker so that the Qe increases.

E. Coupling coefficient extraction

The coupling between two resonators depends on the distance which separates them. Indeed, when two resonators are close to each other, their resonances are disturbed because of the coupling that connects them. The HFSS simulator is used to calculate the resonant frequency of even and odd modes. The inter-resonator coupling coefficient, noted (k), is given by the following formula:

$$K = \frac{f_2^2 - f_1^2}{f_2^2 + f_1^2}. \quad (13)$$

To extract the cross-coupling between resonators 1 and 4 from the filter configuration in Fig. 10 we use a layout of the figure for EM simulation. In this case, the coupling between them is dominated by the electric field and hence, is called electric coupling. This implementation of cross coupling is necessary because M_{14} and M_{23} must be of opposite signs to achieve a pair of transmission zeros at finite frequencies. The

frequency response of the structure in the simulated Fig. 11 below shows the two resonance peaks used to evaluate the coupling coefficient between the first and the fourth resonator.
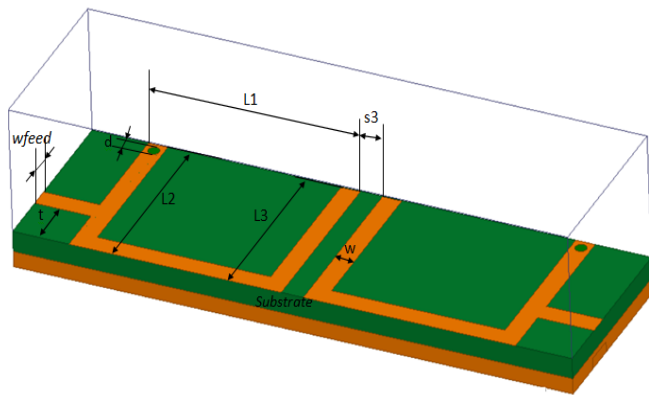
Fig. 10. Arrangement for extracting coupling coefficient M_{14}
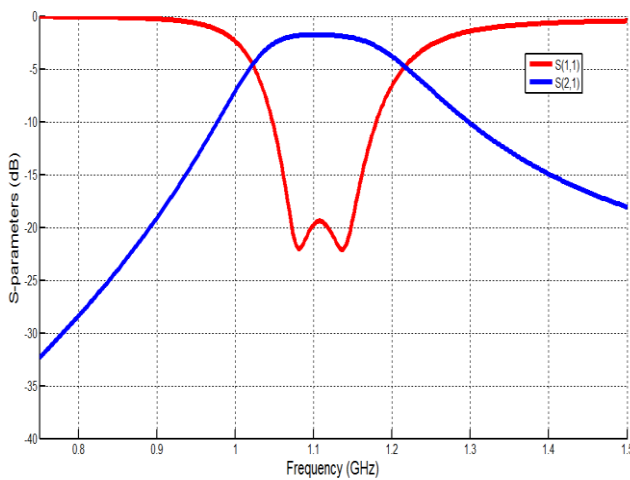
Fig. 11. Electromagnetic response of the 2nd order bandpass filter.

F. Effects of variation of the spacing S physical parameters on UBW-BPF:

All optimized physical dimensions of a proposed cross-coupled MSL-UWB band pass filter operating at 1.2 GHz are obtained by parametric study geometry shown in Fig. 5. the nature of variation of filter S parameter characteristics is studied and analyzed for the variation of one physical parameter while keeping parameters constant, in order to obtain the best optimized physical dimensions of the geometry, which can best meet the low insertion loss and return loss such as more than 10 dB return loss over the entire bandwidth [10]. The first parametric study shows the sensitivity to the variation of the physical parameter S_1 on the parameters S as a function of the frequency plot is illustrated in Fig.12. As the value of S_1 increases from 0.6 mm to 1.2 mm, the performance of S parameters is deteriorates in the frequency band 1.15 GHz to 1.3 GHz. When the value of S_1 is equal to 1.2 mm, the filter has narrower passband region (in the frequency band from 1.15 GHz to 1.3 GHz), its bandwidth becomes wider as the value of S_1 is equal to 0.9 mm.The adverse effects can be specifically observed on the S_{11} (reflection loss) performance for a value of $S1$ being less than

0.9 mm. Therefore, the optimized value of S_1 is chosen as 0.9 mm, considering the performance of S parameters in both bands. For the $S_1 = 0.9$ mm version, the overall bandwidth remains almost constant, from 1.15 GHz to 1.3 GHz.
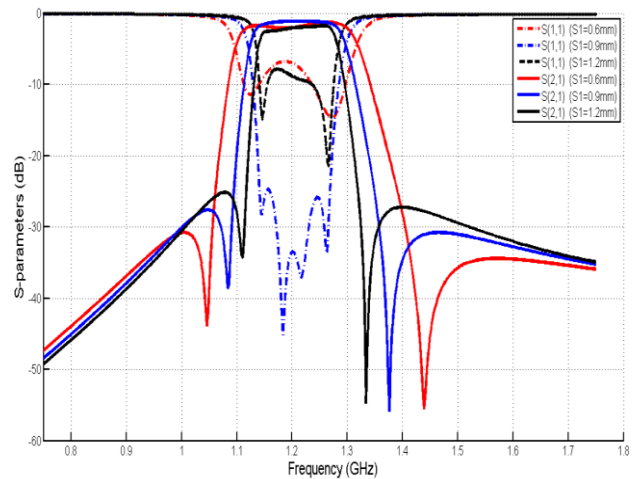
Fig. 12. Simulated results proposed of the filter with different values of S_1

Fig. 13 shows the effects of changing the physical parameter S_2. The optimal value of S_2 is considered to be 0.1509 mm. It can be seen from Fig. 13 that as the value of S_2 increases from 0.150 mm to 0.350 mm, the S parameters are improved in the frequency range from 1.1 GHz to 1.35 GHz. Therefore, the value of S_2 is considered as 0.25 mm by compromising the performance in passband.

Fig. 14 illustrates the simulation results S_{11} and S_{21} proposed with different values of 'S_3' increasing from 1.316 mm to 15.16 mm. This parametric study shows the influence of the 'S_3' spacing between first and fourth resonator. As the 'S_3' gap increases, the upper cutoff frequency and the band gap point are shifted slightly downwards, which means a narrower bandwidth. Considering the response of the S parameters in the band 1.15 GHz to 1.3 GHz, the value of S_3 is chosen to be 1.316 mm.
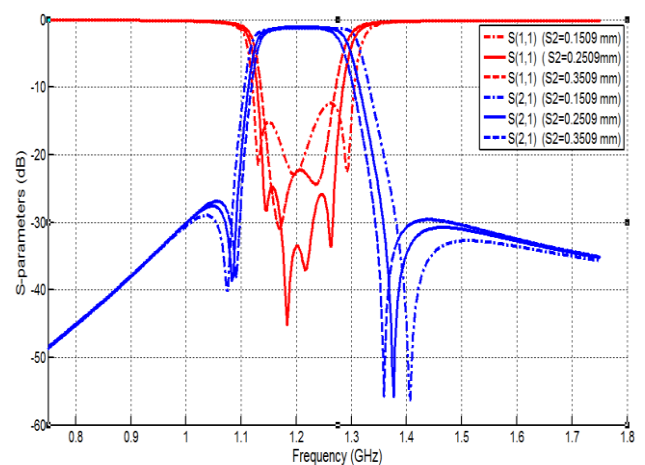
Fig. 13. Simulated results proposed of the filter with different values of S_2
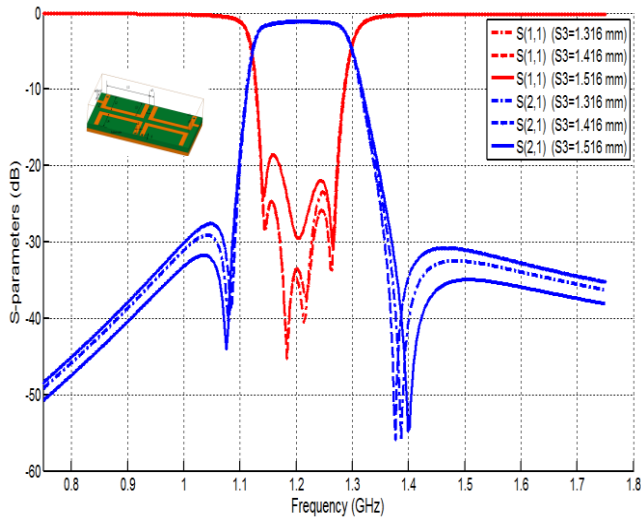
Fig. 14. Simulated results proposed of the cross bandpass filter with different values of S_3

Fig. 15 compares the simulated response of the proposed four pole microstrip bandpass filter after the to the ideal coupling matrix response that shows excellent agreement to the ideal response. In Fig. 15, the proposed filter has reached a filtered bandwidth from 1.13 GHz to 1.28GHz with a center frequency of 1.2 GHz. In the passband [11], the insertion loss is about -1.1 dB and the return loss is less than -24.7 dB and can reach -44.9 dB at the frequency of 1.18 GHz [11]. The comparative S-parameters versus frequency response of the EM simulation and circuit model are shown in Fig.15. The EM simulation results correspond to the optimized physical parameters listed in Table 4. the loss frequency bands-3 dB insertion for EM simulation and circuit model are 1.15 GHz to 1.3 GHz and 1.14 GHz to 1.3 GHz, respectively. The passband insertion loss in less than 1.14 dB and 0.01 dB respectively and the reflection loss is less than 24.5 dB and 25 dB respectively for EM simulation and circuit model. The EM simulation results show good stopband rejection ($|S_{11}| < $ -30 dB and $|S_{21}| < $ -0.21 dB) from 1.375 GHz to 1.75 GHz and strong decrease in bandwidth at the stopping strip. The fractional bandwidth of the filter turns out to be 12.84%.
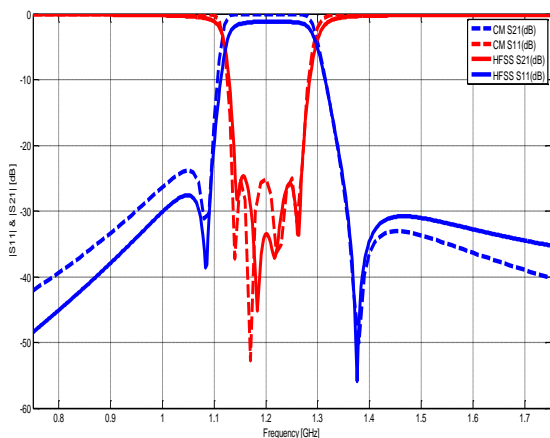
Fig. 15. Simulated results of the filter, in comparison with the ideal responses plotted from the coupling matrix

Fig.15 compares the simulated response of the proposed four pole microstrip band pass filter after the to the ideal coupling matrix response that shows excellent agreement to the ideal response. Outside the filtered band, good rejection is obtained with an attenuation of more than 30 dB at the frequency of y1.08y GHz and the rejection is more than 50 dB at the frequency of y1.37 GHz. The designed filter exhibit desired frequency response with the two finite transmission zero as expected. The electric field distribution of the proposed bandpass filter is shown in Fig.16.
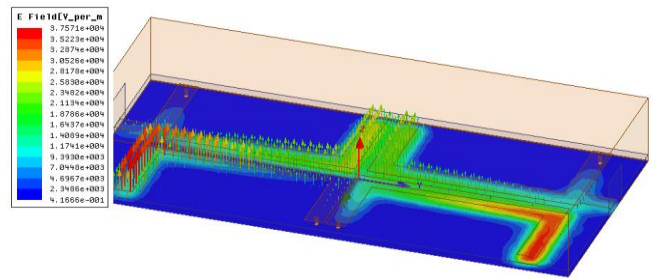
Fig. 16. Distribution of the electric field at 1.2 GHz

In the order to obtain the group delay performance of the overall fourth order filter, the phase values of S_{11} and S_{21} are calculated in HFSS as a function of frequency, which are demonstrated in Fig. 17. Then, the values of simulated group delay as a function of the frequency of the proposed cross-coupled bandpass filter are obtained.

The simulated group delay as a function of the frequency of the proposed cross-coupled bandpass filter is shown in Fig. 18. The high and variant group delay response can be observed throughout the band width of the UBW-BPF. The simulation and group delay varies between 0.1 ns and 4.5 ns [12]. The maximum variation of the simulated group delays is 4.5 ns. However, a relatively large constant of group delays in the simulation results can be observed at both ends of the bandwidth, which occurs due to the abrupt transition of the insertion loss curve from the bandwidth to the stopping strip. Strong group delay response throughout the operating frequency bandwidth shows the correct time domain.
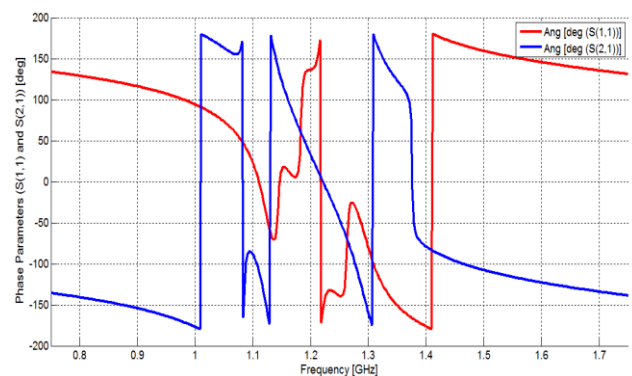
Fig. 17. Frequency response (Phase) results of the cross bandpass filter

A performance comparison between the proposed work and the recently published works are given in Table 4. According to this table, the proposed microstrip filter has good parameters, such as low values of insertion loss and high isolation between two channels at the operating frequencies,

which is a very important factor in modern communication systems [12]. Therefore, the proposed circuit has a relatively better overall performance, compared to the other filters.
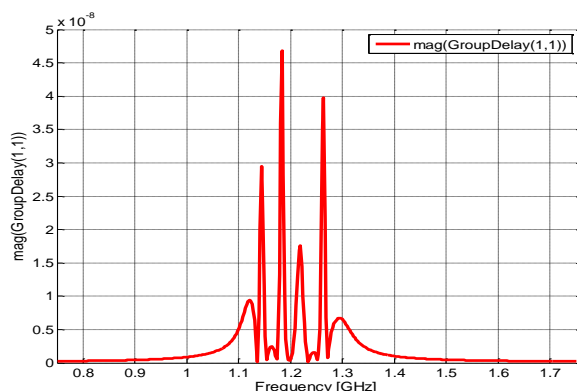
Fig. 18. Group delay of a microstrip resonator

TABLE 4.
PERFORMANCES OF THE PROPOSED MICRO STRIP FILTER AND THE RECENTLY PRESENTED MICRO STRIP FILTERS

Refs.	Order	Frequency (GHz)	Return loss (RL) dB
[10]	04	1.26	18 dB
[12]	03	0.9	20 dB
Work in HFSS	04	1.20	25dB
Work in AWR	04	1.20	25 dB

IV. CONCLUSION

This work based on the design and development of a cross-coupled bandpass filter using an RLC resonator combined with a TL transmission line are presented in this paper. The RLC resonator with TL is designed for unit cell coupling of RLC-TL. The filter is small with a size of $25 \times 52 \times 0.83$ mm^3 and excited by a microstrip line (MSL) as well as calculation of various synthesis parameters of a cross filter (the coupling Matrix the Quality Coefficients) [14]. According to the introduction of transmission zero, the simulations carried out by the AWR (Microwave office) software are closely correlated to the HFSS simulation results with a central frequency of 1.2 GHz and a reflection coefficient (S_{11}) less than 25 dB in the bandwidth. Thus, a very good consistency between the curves of the HFSS simulations and those produced by the AWR software leads to the development of a high performance filter structure for modern multiservice communication systems with an insertion loss of 0.21 dB and -25dB return loss across the entire bandwidth from 1.15 GHz to 1.35 GHz with a bandwidth fraction of 12.83%. Additionally, the filter also exhibits a group delay response (4.5 ns maximum deviation) and varies across the entire bandwidth. Finally, very good consistency between the curves of the HFSS simulations and those produced by the AWR software leads to the development of an efficient filter structure serving mobile communication applications.

Due to its small size and good performance, the proposed BPF can be used in modern small-scale wireless communications systems. Since the filter is based on microstrip structure, which has relatively moderate power handling capacity, its usage in the practical applications is more proper for receiver channels of communication systems at which low RF power is propagating. Since the received power is low in the receiver channels, this filter can play a critical role for the suppression of additional noise and interference coming from out-of-band regions. Besides, these systems usually need transmission zeros in the filter/transmission response at the frequencies close to lower and upper edges of passband region, which eliminates possible high interference coming from these frequencies. The selected passband region of 1.15 – 1.35 GHz of the proposed filter occupy several L-band mobile and wireless communication systems in the fields of aeronautical radionavigation, radionavigation satellite [15], radiolocation and amateur radio. GPS (lower L-bands of L2 and L5 bands) and Galileo (lower L-bands of E5 and E6 bands) satellite navigation systems commonly used for civilian and military positioning, L-band radar altimeters used to measure altitude above the ground or sea surface, radio sensing (weather radars) and radio astronomy can be some of the practical applications at which the proposed filter can be used. By changing the centre frequency of the filter, the structure can be modified and used in different RF and microwave applications. The future research of the study can be directed to the realization and verification of the designed filter with manufacture and measurement results. Besides, the increase in the order of the filter for the applications, where sharper (higher) rejection is needed at the out-of-band regions, can be handled. The usage of the coupling matrix method can be investigated for higher filter orders of the proposed filter.

REFERENCES

[1] K. R. Jha and M. Rai, "A Slow Wave Structure and Its Application in Bandpass Filter Design", *AEU-International Journal of Electronics and Communications,* vol. 64, no. 2, pp. 177-185, 2010, DOI: 10.1016/j.aeue.2008.12.005

[2] B.-A. Twumasi and J.-L. Li, "An Equivalent Circuit Model of a Rectangular Bracket Shaped DGS and Its Microwave Filter Applications", *Journal of Electrical Engineering*, vol. 70, no. 1, pp. 32-38, February 2019, DOI: 10.2478/jee-2019-0004

[3] W. Feng, C. Wang, R. Gomez-Garcia, and W. Che, "Single-Ended-To-Balanced Balun-Based Dual-Band Power Divider With Open-Ended Stubs", in *2018 IEEE MTT-S International Wireless Symposium (IWS)*, 2018: IEEE, pp. 1-3, DOI: 10.1109/IEEE-IWS.2018.8401007

[4] W. Xia, "Diplexers and Multiplexers Design by Using Coupling Matrix Optimisation", *School of Electronic, Electrical and Systems Engineering*, University of Birmingham, 2015.

[5] J. Zhou, M. J. Lancaster, and F. Huang, "Coplanar Quarter-Wavelength Quasi-Elliptic Filters Without Bond-Wire Bridges", *IEEE transactions on microwave theory and*

techniques, vol. 52, no. 4, pp. 1150-1156, 2004, DOI: 10.1109/TMTT.2004.825706

[6] Z. L. Zhu, and J. L. Li, "Design of Dual-Mode Loop Resonator-Based Microwave Diplexers with Enhanced Performance", *Radioengineering*, vol. 31, no. 4, pp. 527-532, Dec. 2022, DOI: 10.13164/re.2022.0527

[7] M.-H. Weng, S.-W. Lan, S.-J. Chang, and R.-Y. Yang, "Design of Dual-Band Bandpass Filter With Simultaneous Narrow-and Wide-Bandwidth and a Wide Stopband", *IEEE Access,* vol. 7, pp. 147694-147703, 2019, DOI: 10.1109/ACCESS.2019.2946302

[8] I.-H. Kang, K. Wang, and S. M. Li, "Modified Compact Combline Filter Using Planar Parallel Coupled Structure with Extended Rejection Bandwidth", *Journal of Navigation and Port Research,* vol. 34, no. 7, pp. 543-552, 2010, DOI: 10.5394/KINPR.2010.34.7.543

[9] K. Becharef and K. Nouri, "Miniaturization of SIW Broadband Bandpass Filters Based on the Complementary Interdigital Resonator E (CIRE)", *Wireless Personal Communications,* vol. 125, no. 1, pp. 649-664, 2022, DOI: 10.1007/s11277-022-09570-9

[10] M. Damou, M. Chetioui, S. Gouni, A. Boudkhil, R. Bouhmidi, and B. Bouras, "Optimization of Multi-Ports Combline Filter Using Admittance Extraction Technique", in *2022 International Conference of Advanced Technology in Electronic and*

Electrical Engineering (ICATEEE), pp. 1-5., 2022, DOI: 10.1109/ICATEEE57445.2022.10093720

[11] J-L. Li, K-X. Song , L-F. Jiang , J-P. Yang , S-Q. Zhou, "Dual Mode Bandpass Filter With Switchable Response", *Journal of Electrical Engineering*, vol 74,no 2, pp.137–139, February 2023, DOI: 10.2478/jee-2023-0019

[12] S. S. Gao , J-L. Li , Z. L. Zhu , J..L Xu, Y. X. Zhao, "Dual-Mode Resonator Filter With Improved Feed-Lines for Dual-Band Applications", *Journal of Electrical Engineering*, vol 71,no 6,pp. 433–435, December 2020, DOI: 10.2478/jee-2020-0060

[13] G. Lee, B. Lee , J-Y. Jeong, and J. Lee, "Ka-Band Surface-Mount Cross-Coupled SIW Filter With Multi-Layered Microstrip-to-GCPW Transition", May 23, 2019, date of current version June 4, 2019, DOI: 10.1109/ACCESS.2019.2918588

[14] G. Lee, B. Lee, J. Y. Jeong and J. Lee, "Ka-Band Surface-Mount Cross-Coupled SIW Filter With Multi-Layered Microstrip-to-GCPW Transition," in *IEEE Access*, vol. 7, pp. 66453-66462, 2019, DOI: 10.1109/ACCESS.2019.2918588

[15] A. Rezaei and L. NOORI, "Tunable Microstrip Dual-Band Bandpass Filter for WLAN Applications" *Turkish Journal of Electrical Engineering and Computer Sciences*, vol 25, no 2, pp. 1388-1393, 2017, DOI: 10.3906/elk-1508-217